

CAD Numerical-Polynomial Refinements in Vertebral Bone Surface with Geometrical Data Development for Surgical Devices Design

F Casesnoves MSc (Physics) MD

Computational Bioengineering Researcher

IIS International Institute of Informatics and Systemics (Individual Researcher Member)

Orlando, Florida State, USA

casesnoves.research.emailbox@gmail.com

Abstract. The bioengineering design of surgical instrumentation to exert forces and torques/moments on bones/tissues during operations depends on the mechanical adaptability/efficacy of these tools. In previous contributions [refs 5-11], it was presented a mathematical-computational method to obtain the shape-geometrical equations of the of lumbar spine, in order to use this data for surgical instrumentation design/manufacturing. We developed in this contribution a further polynomial numerical-refinement to enhance the accuracy both of the CAD images of vertebrae and precision of the polynomial equations of lumbar spine anterior shape. The mathematical method was the discretization of the original scanning-data of each vertebra to reduce numerical-fitting errors, since the surface was divided into several subsections/discretized-zones. After that mathematical task, fitted-subdivisions are computationally joint to get a complete image/improved-equation of the vertebral anterior surface. The results agreed to formal numerical analysis theory and provided with better vertebral CAD representations that show a more realistic images of lumbar spine. Therefore, we proved that discrete-approximations for bone-surface give better precision/accuracy in mathematical-shape equations used for instrumentation design. Clinical applications examples, related to former publications [refs 5-11], were presented for manufacturing of surgical spinal distractors, which can be extrapolated for the bioengineering design of other types of vertebral surgery tools.

Keywords: ROI (Region of Interest), simulations, nonlinear optimization, fitting, least-squares method (LSM), least-squares algorithm (LSA), inverse analytic approximation method, computer aided design (CAD), Discrete Numerical Approximations.

I. INTRODUCTION

Spinal surgery constitutes a high risk speciality among the surgical disciplines. Such risk is due to the proximity between the operating field, and peripheral nervous system tissues, such as the spinal cord, important emerging nerves branches, and vascular structures. Currently, the use of different prostheses and artificial implants (rigid and non-rigid) in spinal surgery is increasing. Furthermore, these technical alternatives, carried out with different instruments, have become more frequent and specialized. Consequently, the new design of surgical instrumentation should take into account a number of essential conditions for the improvement of the surgical work at theatre. The instrumentation in contact with the bone, to exert mechanical forces and torques/linear momentums, should apply the minimal force to obtain the desired effect. An additional objective is to design each instrument so as not to interfere with surrounding anatomical structures or any other surgical tool(s) within the operating field, and provide with the conditions for a fast/precise intervention. In addition, the

tools should be suitable for quick/large-force-range maneuvers, and their size has to be adequate. Therefore, the efficacy/precision of the new instruments is determined by the condition that no failed maneuvers/delays/patient-compromise could occur, and the surgeon experiences a balance between strength, effect, optimal forces, and fast efficacy.

According to these conditions [refs 5,6], precise meshing between the instrumentation and the exterior bone boundary is essential for biomechanical efficacy. Surgical instrument design must meet these conditions. But this optimized design is difficult for several anatomical and pathological factors. First, the complex anatomical bone surface, and morphological differences related to age, ethnic origin, body frame, and sex, are significant. In addition, the degenerative and traumatic processes of the spine (such as arthrosis, osteophytes of different grade, arthritis, or injuries), can cause additional irregularities in bone surfaces with shape variations. To attempt to resolve these problems, the modeling (CAD) of the bone morphology, becomes crucial in bioengineering. CAD allows simulating and carrying out reliable statistic for the instrumentation design and manufacturing. But the digital computers work with large-scale digital data, and discrete approximations become necessary [9]. This is the field of the Numerical Geometry, that deals with representations, data structures, and algorithms related to geometrical objects. Given a large sample, the inverse problem used by computers, is to obtain a discrete shape for the object. The forward problem is, given a defined surface (discrete or analytically), obtain any object representation. CAD Modeling is a crucial method in Bioengineering to resolve the complicated bone morphology problems [refs 1-5]. CAD allows simulating and carrying out reliable statistical analysis for instrumentation design and manufacturing.

Primarily, this paper shows previous developments [refs] of an innovative simulation to convert a point cloud from 17 natural specimens, into surface representations of the anterior vertebral body. Subsequently, ROIs divisions of these 3D vertebral surfaces were fitted to a second-degree polynomial model which conforms to the initial natural ROIs, getting low error ratios. By using this model as an initial step, the complete Inverse Approximated Discrete Problem was carried out, from the digitalized points to a Delaunay shape, with a final approximation to obtain the surface refinement analytical equations. That is, we used

further subdivisions for each vertebra/ROI [Figs 1,8-12], to obtain a more accurate representation of the vertebral shape. Results show improvements both in CAD imaging and agreement to the real vertebral geometry. We presented in this contribution a series of computational images that put forward the acceptable mathematical refinement as a primary stage of imaging approximation method to be improved in next publications. We also present a practical engineering application [Appendix, 3], for the design of a lumbar spine distractor, which can be provide with an innovative technique for vertebral distraction and related spinal surgery maneuvers. To summarize, this article is focused on further computational improvements in CAD and vertebral-shape equations deduction through nonlinear optimization polynomial refinements.

explicit equation with only the variable Z on the left hand. That is, to sum at both sides of the equality convenient constants to form a perfect Z-square binomial at the left side. However, with this variable change, a square root gives the final value for Z. This implies that, when the fitted ROI was visualized with griddata, negative numbers into the square root could appear, generating a final complex value for Z. These complex numbers can be obtained on the extremes of the fitted ROI, because in that part of the ROI, the numerical approximation becomes very tight. The solution to avoid this inconvenience was to select only the absolute values of the root in the visualization program [Eqs Fig 2]. Recently, new available software permits also to sort this kind of difficulties. A second question arose when the size of the ROI rectangle was chosen.

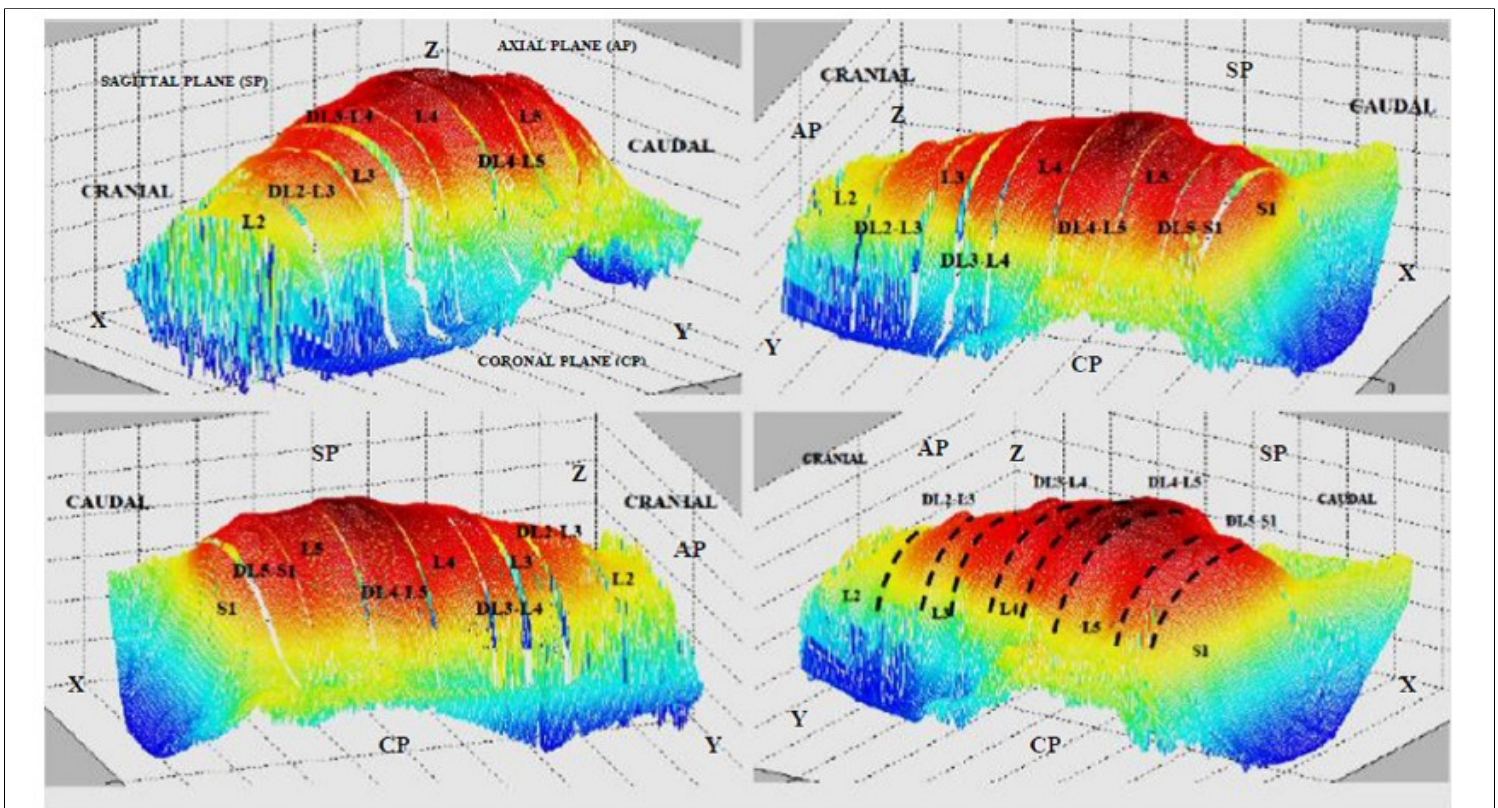


Fig 1.-A CAD of a cadaveric lumbar spine (Special software to separate each vertebra, previous publications)). Anatomically described for sharp learning as a base to interpret the new numerical methods of this contribution.

2.-MATHEMATICAL METHOD

We explain initially the mathematical method used for ROI computational extraction in previous work [refs 5-7]. It has been extensively presented in the Literature, the usual least-squares formula for a non-linear 3D fitting and its error calculation approximations. Because of a classical hyperboloid formula was implemented, it was strictly necessary to make the Z variable explicit to set the algorithm properly. We carried out a simple Z-translation [Eqs Fig 2], and variable change steps that were used to obtain an

The vertebra surface is curved, and the values of the rectangle that forms the ROI, and are given by the visualization Matlab tool, are over the XY plane. Therefore, if we need a rectangular ROI of about 35mm long, the 35mm side of this rectangle is formed by a geodesic, not a straight line. Then, the projection of the geodesic length is less than 35mm [Appendix 2]. It is necessary to calculate the approximate length at XY plane, that corresponds to that geodesic-side of the ROI which is 35mm long. This difficulty was solved with a 2D parabolic fitting, of the geodesic that defines the rectangle longer side, since its shape was nearly parabolic for all the spine samples. Once this geodesic parabolic equation is known, we can calculate the integral limits of the curve that define a curve length of about 35mm. This was done with a simple optimization program, and the projection length at the XY plane resulted

to be about 30mm. The short rectangle side (~10mm) projection, can be approximated to a straight line of about 10mm long at the XY plane. With this step, the mathematical development concludes at all. In **Equations Order, Fig 2**, we show synthesis of the mathematical development that was carried out to prepare the algorithm function for a feasible programming. The constants K_i included in these formulas, constitute the parameters whose optimal values are going to be obtained with the designed software. The upper equation is the classical Hyperboloid formula of Analytic Geometry, with the vector \mathbf{X}_0 that defines the 3D Center Position. We see on the lower equations, the Z translation with a variable change to make this Z variable explicit. Note the square root on the right side, that complicates the visualization program results, because it generates complex numbers during the Computational Optimization. The lowest equation is a concise formulation of the Optimization Objective Function, without constraints, that has been implemented.

It is recommended to read briefly some mathematical references, to catch an idea of the accuracy and results that the programmer can expect by using this classical method.

Least-squares (LS) method for optimization, and inverse nonlinear optimization has been extensively presented and developed in the literature. We used in this paper, as usual, L_2 Norm to carry out the objective function algorithm, and basically the same mathematical method than in previous publications. In Fig [2], it is shown the previous polynomial-fit development of the objective function. As a reminder [refs 5-11], we show in Appendices 1 and 2 explicit figures/tables of numerical results obtained in non-refined polynomial optimization with geometrical projections.

2.1.-COMPUTATIONAL-GEOMETRY ALGORITHM WITHOUT REFINEMENT

The non-refined numerical fitting was implemented (Matlab) with a LSA without constraints, a discrete L_2 Norm, and specific software for lsqnonlin routine. Lsqnonlin uses the Interior-Reflective Method, appropriate for nonlinear programming. It is intuitive to see the resemblance between the hyperboloid (2nd degree polynomial) and the facets of the vertebrae. The refinement was carried out with Frenet Subroutines, by using formal optimization methods.

$$\frac{(x - x_0)^2}{a^2} + \frac{(y - y_0)^2}{b^2} - \frac{(z - z_0)^2}{c^2} = 1$$

and,

$$\vec{X}_0 = (x_0, y_0, z_0)^T$$

$$z^2 + k_1 z = k_2 + k_3 x + k_4 x^2 + k_5 y + k_6 y^2$$

$$(z - z_0) = (k_1 + k_2 x + k_3 x^2 + k_4 y + k_5 y^2)^{1/2}$$

Objective Function,

$$\sum_{i=1}^N \left\| (z_i^2 + k_1 z_i) - (k_2 + k_3 x_i + k_4 x_i^2 + k_5 y_i + k_6 y_i^2) \right\|^2$$

Fig 2.- Nonlinear Optimization Formulas.

Above, Fig 2, we showed the equation that was used for non-refined fitting. The same mathematical formula can be used for each discretized zone/volume.

2.1.1.-COMPUTATIONAL OPTIMIZATION

As said, the numerical fitting was implemented with a least-squares algorithm without constraints [Fig 2]. The optimization process was carried out by using a discrete L_2 Norm, and specific software designed for lsqnonlin subroutine. All the fitted ROIs were visualized with griddata [Figs. 6,7], to check the precise resemblance with the corresponding natural ROI. The intuitive way to see the resemblance between the classical 3D hyperboloid and the anterior facets of the vertebrae is shown in Figs. 3,6. It displays a basic scheme that represents the evident resemblance between the 3D classical hyperboloid surface, and the anterior vertebral body geometry. This resemblance was the starting point to try a second degree polynomial fit. On the right, a front view of a lumbar vertebra, showing the anterior facet, to see better the similarity of the conformal surface.

2.1.2.-MATHEMATICAL -COMPUTATIONAL DEVELOPMENT DETAILS FOR CAD IMAGING CONSTRUCTION WITH CADAVERIC DATA/SPECIMENS

The simulations of the anterior vertebral body are based on 17 human cadaveric samples. The cloud data of these cadaveric samples was obtained with a 3D Scanner Digitizer. This number of cadaveric samples is just the group of anatomic specimens that were available for this experimental purpose. The coordinates frame used to get the cloud data was the same for all the lumbar specimens. The cloud data of the anterior surface of the lumbar spines which was obtained, had about $\sim 10^5$ digital points for each individual spine. It was necessary to reduce the initial points number from $\sim 10^5$ to $\sim 10^4$ in order to run quicker the visualization programs. The points cloud was also translated to set them centered about the 3D coordinates origin [Fig. 1]. The first programs series developed with griddata subroutine were made to visualize the complete 17 lumbar spines one by one [Fig. 1]. This kind of developed software is relatively simple, and its only time-consuming inconvenient was to load and order a large matrix that contains all the cadaveric sample points ($\sim 10^4$) [Fig 1]. The definition of the size of the grid when editing the program code, is also important, because it has consequences in the number of fitting approximated points, the optimization residual, and error values. When visualizing each individual spine sample with

the software, it was observed significant irregularities, both natural (such as different vertebrae sizes, or variation of curvature of the lumbar spine), and pathological (signs of arthrosis, osteophytes, and shapes corresponding to intervertebral disc degeneration).

We show in **Fig. 1.**, a visualization of a complete anterior lumbar spine cadaveric sample. On the right, a lateral view, displaying the vertebrae (from left to right) L3, L4, L5, and S1, with the corresponding intervertebral discs. On the left, a frontal sketch that was made for the caption of the L3 vertebra. Note that the scale of the axes is different, and in the reality, the anterior lumbar spine is almost plane. The following second type of developed programs were designed to extract the so-called Region of Interests (ROIs) of the anterior vertebral body surface [**Fig. 3**]. These ROIs constitute the parts of the vertebral body surface that keep in contact and mesh the surgical instrumentation, in our particular case, a vertebral spine distractor. The ROIs were rectangular strips (35mm x 10mm) of the anterior vertebral surface, at a distance from the superior or inferior endplate of about 10mm. To carry out a ROI selection, the coordinates that limit this rectangle are found over the image of the total spine surface, by using the image tools available provided by the software. For this purpose, given the obtained coordinates that set the limits for the rectangle, we seek the corresponding place (row and column numbers), of these coordinates into the resulting matrices of the initial designed program. Then, we load only these matrices points of the ROI into a second griddata program, to visualize the selected ROI and observe its curvature and possible irregularities (which is very frequent). In **Fig. 3**, it is shown a typical natural ROI that has been obtained with the second implementation of the griddata subroutine. The synthesis of the programming code with our software for the complete spine is on the lower **Fig. 7**. Therefore, the natural ROIs surfaces have already been separated and delimited properly. These natural ROIs have to be fitted into a mathematical equation to carry out the realistic simulations. A second degree polynomial model was chosen for the fitting. The reason for it was the significant resemblance between the classical 3D hyperboloid equation, and the shape of the anterior vertebral body surface. In the following Section of Computational Optimization, the complete optimization technique that was made for this numerical fitting is presented in detail. Recently, algebraic-geometry work/equational-methods has been published related to hyperboloid irregular/variable geometry [SIAM Proceedings of ref 10].

2.2.-REFINEMENT NUMERICAL METHOD (I)

The usual non-refined Least Squares Method for a nonlinear fitting and its error approximations, has been extensively presented in the literature [e. g. ref 1]. Because a hyperboloid formula was implemented, it was necessary to make the Z variable explicit to properly set the algorithm. We carried out a Z-translation, and variable change steps to

obtain an explicit equation with only the Z on the left. That is, summing to both sides of the equality convenient constants to form a complete binomial on the left. Consequently, using this change, a square root gives the final Z value. Then, when the fitted ROI is visualized, we could get complex values for Z. These complex numbers sometimes are visible in the ROI as upturns in the curvature at the edges. We show in the next slide a natural Delanuy vertebral fit compared to a polynomial fitting without refinement.

For polynomial refinement, we work initially with a 2 and 4 zones-steps refinement for any vertebral surface (Figure 5). The theoretical framework of the refinement is based on the decrease of residuals and errors when we reduce the number of data points to carry out a CAD image of a vertebral region. Analysis of this kind of fitting-refinement with standard determination coefficients will be presented in subsequent publications.

2.3.-REFINEMENT NUMERICAL METHOD (II)

This subsection is intended to show graphically two ROI computational software results, both in Matlab (previous contributions) and Freemat. Later on subsection 2.4, we will discretize these ROIs with numerical refinements.

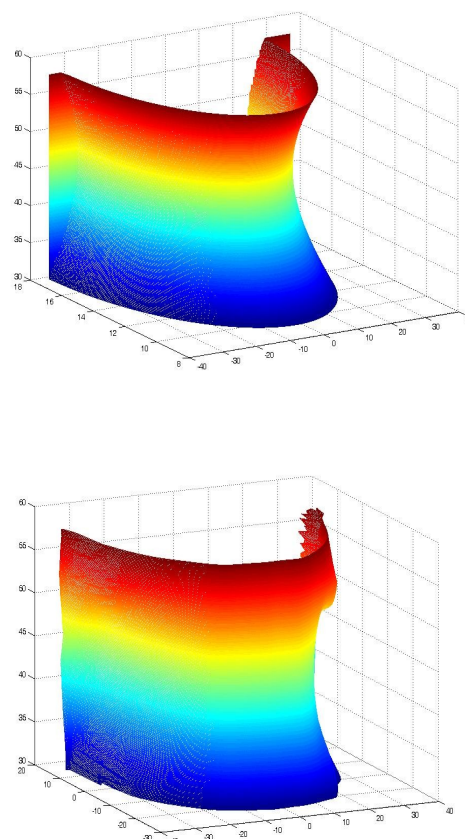


Fig 3.-Classical images. (upper polynomial-fitted, and lower Delanuy natural picture). We work with ROIs selected, not with the complete vertebral body.

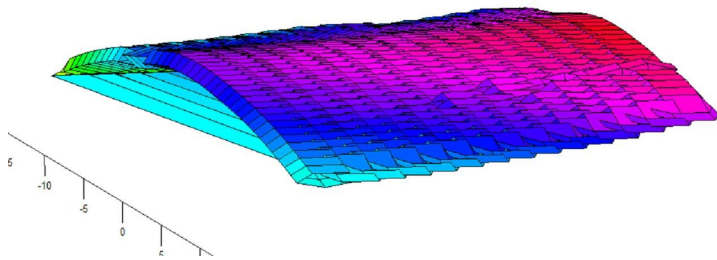


Fig 4.-An image of a ROI obtained with Freemat Surf Subroutine. Note the differences between Matlab and Freemat related to image computational construction and use the different colors to link coordinates with corresponding parts of surface.

2.4.-REFINEMENT NUMERICAL METHOD (III)

Development of mathematical refinement has a number of computational-numerical steps. The basic refinement technique is to divide the surface cloud points (one vertebra) in several discretization zones/voxels/pixels. Each zone (vertebra) is treated for a polynomial fitting independently (3D, voxels of cloud data). We fit the cloud data of each voxel to a polynomial, and after that we carry out the development of the polynomial for the voxel zone/volume coordinate limits to obtain a fitted polynomial point cloud. This resulting clouds for each pixel/voxel can be visualized as a surface of the vertebra in a unique image.

Computationally, (Freemat or Matlab), it is imperative to carry out a series of matrices data selection to make a further-refinement subdivision. Whether for the complexity of cadaveric data, or the biased scanning-values that we can find in this task, the refinement becomes difficult with relative frequency.

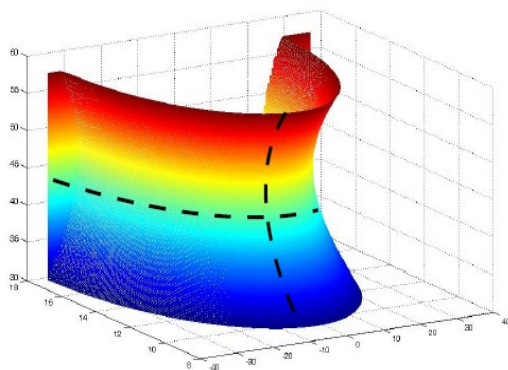


Fig 5.- Discretization Method. (Subdivision in Bisections)

(2-zones), or Quadrants (4-zones). Note that the subdivisions not necessarily have to be totally symmetric.

We used, pictured Fig [5] as starting point the fit for the total region, and then this equation was corrected for each zone (bisection or quadrant). The chosen region/equation was the average upper L5 zone used in previous publications (Ref 1, see table of equations, pictured here).

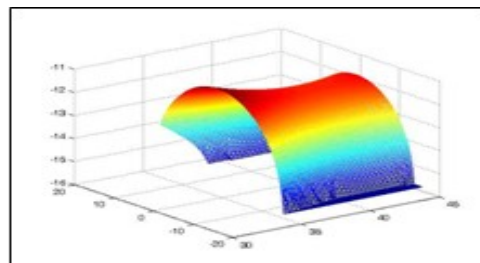
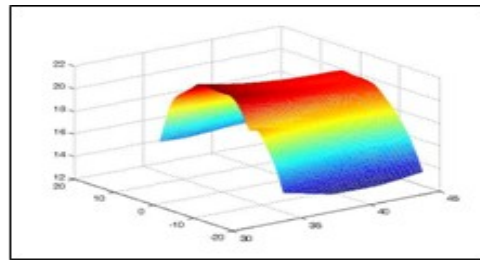


Fig. 6-We show a comparison between a natural ROI of lower L5 surface (upper), and the fitted ROI (lower). We see how the natural curvature has been kept by the fitting (along X Axis), and the general shape is very similar.

3.-COMPUTATIONAL SOFTWARE

Several subroutines of Freemat 4.2 (Samit Basu, General Public License), were used to carry out the numerical fitting and the 3D surface images. The least-squares residuals are automatically obtained with the subroutines commands. To obtain a 3D image of both a discretized zone [figs] and the complete anterior vertebral surface [figs], basic 3D plotting subroutines of Freemat were applied, e.g., Surf, Polyfit, Meshgrid etc. The matrices changes and matrices reshape were also required in software development. In general, the polynomial fit is not too complicated provided we start with the total region fitting.

The subroutines to fit polynomials in Freemat were used to get a numerical fitting for each discretized zone of the vertebra. There are subsequently several subroutines to implement the fitted points into a 3D surface. Images of the sum of discretized zones/volumes can be joint in a unique image simply adding all the fitted points within a matrix. The implementation of imaging CAD in Freemat is similar to Matlab [Fig.7], and we show a simple program for one matrix scanning data point in Matlab that was designed in previous contributions.

```

A=[71.039 -40.362 0.202          b1=max(y) ;
65.328 -38.234 5.672];          steps1=a:0.8:b;
x=A(:,1);                        steps2=a1:0.8:b1;
y=A(:,2);        [XI,YI]=meshgrid(steps1,steps2);
z=A(:,3);          ZI=griddata(x,y,z,XI,YI);
a=min(x);          mesh(XI,YI,ZI);
b=max(x);          hold
a1=min(y);         hold off
    
```

Fig. 7-Brief Matlab code of nonlinear optimization program for CAD implementation without refinement [refs 5-8]. This program is extremely simple, and a series of improvements were carried out for previous/present contributions. Of course, matrix A has much more scanning numerical data.

4.-NUMERICAL RESULTS (I)

The **polynomial equation** for the **total zone** is

$$(z - z_0)^2 = 295.82 - 11.3842x + 0.1208x^2 - 0.0339y - 0.0544y^2 ;$$

The **polynomial refined equation** for the **upper bisection** is

$$(z - z_0)^2 (Freemat) = 3243.7467 - 124.8164x + 1.3245x^2 - 0.4375y - 0.5964y^2 ;$$

The **polynomial refined equation** for the **lower bisection** is

$$(z - z_0)^2 (Freemat) = 3149.3397 - 121.1825x + 1.2859x^2 - 0.4247y - 0.5791y^2 ;$$

4.-NUMERICAL-IMAGING RESULTS (II)

We focus, since extent mathematical details were presented in previous sections, in a series of computational imaging pictures to show/prove the refinement approximations objective results. The software of these imaging developments is carried out with Freemat. Note that these images belong to one cadaveric specimen and one vertebral surface, L5, new imaging work will be released in further contributions with corresponding numerical data.

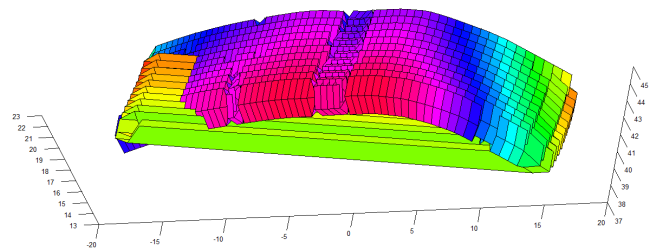
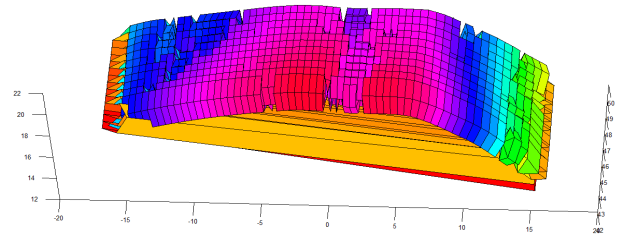


Fig 9 .-The lower (inferior) and the Upper (superior) Natural Bisections of L5 ROI.

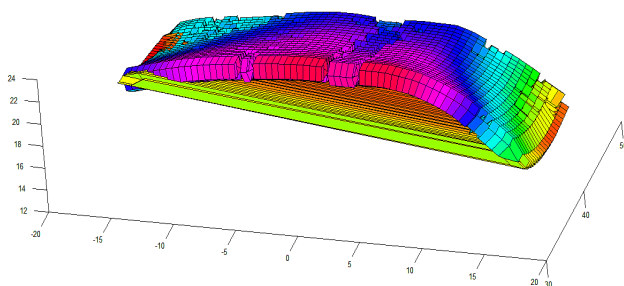
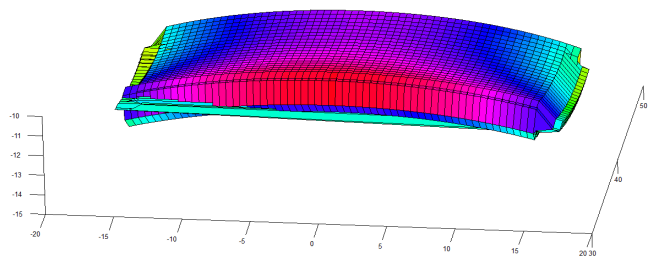


Fig 8.-Pictured, L5 upper natural ROI with Freemat.

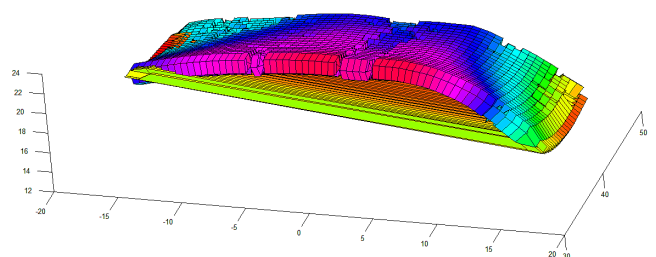


Fig 10.-The Natural (Inferior) and fitted (Superior) L5 ROI.

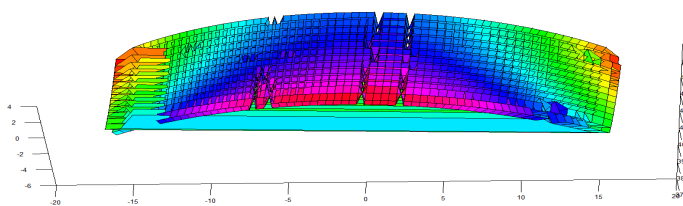
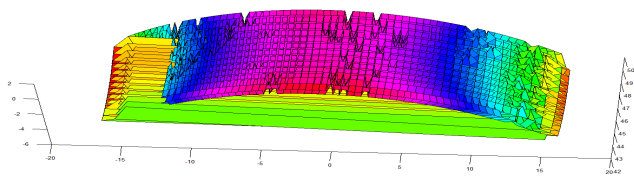


Fig 11.- Pictured, the Lower fitted (inferior) and Upper fitted (superior) L5 ROI. We observe how the Natural irregularities are better reproduced.

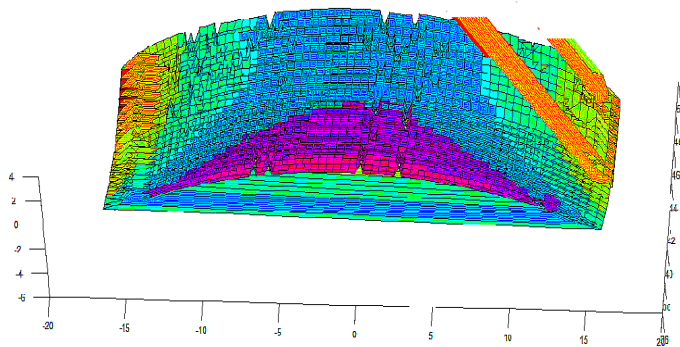


Fig 12.- Here is shown the Upper and Lower fitted sections together, after a computational work that joints in a single image both superior and inferior bisections of Fig 11. The Natural irregularities are clearly preserved.

5.-DISCUSSION AND CONCLUSIONS WITH CLINICAL-BIOENGINEERING APPLICATIONS

Polynomial fitting can be carried out to get a refinement in an initial region that has been divided into several parts. After joining all the fits in every region, we get an overall surface representation with lower error magnitudes. The mathematical reason for this is that the polynomial fit has been reduced and adapted for every region, and therefore there is not a polynomial fitting for all the vertebral surface. As a result, the overall error magnitude decreases, because every region has been adapted to a specific polynomial.

Pictured [Appendix 1], the numerical-geometry calculations that can be used in Biomechanical engineering to design surgical spinal distractors or spinal tools. If we carry out the refinement, the clinical-engineering precision for each region of interest where spinal tools act is increased.

The imaging results can be considered acceptable since the close resemblance between the natural ROIs and fitted ones is evident. This implies clinically that the surgeons, while preparing the intervention, have to evaluate two important matters. First is the spine degeneration grade, for any bone/systemic pathology (we use clinically the term *systemic* to refer general diseases that cause bone-structure alterations/consequences). If the patient is rather old, the disease is chronic/accidental, and the physical exploration gives details of severe bone deformation, combined with acute low back pain/spinal pain, significant mobility limitations, and neurological symptoms, such as radicular pain irradiation and paresthesias, an imaging study is a must. That is, we have sufficient non-interventional data to suspect that the surgical tools have reasonable probability of failure, or at least to find meshing difficulties. Then, it is convenient to carry out a computerized axial tomography (CAT), specialized radiology, MRI study, perhaps SPECT or Impedance Tomography, to see clearly the bone deformations/irregularities of the zone, and especially those bone parts which will receive the distractor screws or invasive parts of the devices or tools. Given this objective information, surgeons can go more prepared to the theater with a wide tool ranged a series of learned images of what they will find within the patient intervention-region, just in case that the meshing of bone instrumentation becomes difficult, select mechanical devices suitable for the operation, or unpredictable circumstances that happen not very infrequently in the daily surgery. The clinical and imaging preoperational information constitutes an essential contribution for the successful outcome, even in the worst cases. This pre-operational information provides in addition with faster intervention time and reduces the high economical cost of a surgical theatre maintenance. Therefore, whether for saving operation time, or getting minimum effort/maximum precision during the intervention (whose outcome is an optimal patient cure), pre-operational imaging study should be always imperative. If time, bioengineering facilities, and budget are available, it could be possible, after an adequate imaging study, or even *in vivo* exploration, to manufacture personalized surgical tools, specific for that difficult patient.

Further possible polynomial refinements to reduce the errors in the future are feasible. One of these methods, is given by the minimization of the partial derivatives of the algorithm, with respect to the polynomial coefficients. This yields a Vandermonde equation whose solution is unique, and can be implemented without important difficulties (the so-called kernel regression method, based on Fredholm integral equations). There are several mathematical methods to improve further this numerical fitting, and we refer the reader to modern/classical nonlinear programming literature where a number of variant methods can be tried to get more

precision/accuracy. Other approaches would be to develop an objective function with a Tikhonov functional ¹, and with/without a penalty term. As a clinical-bioengineering application of the numerical-shape model, we present a surgical distractor designed and shown in Appendix 1, which offers, apart from the optimal positioning of the insertions, the use of four points to apply the force (about 80–150 N each), to widen the intervertebral space by at least 2.5 mm [refs 5-8]. We also can set/illustrate a number of technical comparisons with other distractor types, e.g., Caspar instrumentation. Caspar-type distractors have two screws to apply the force(s). The only distractor that divides the force into four points uses blades, instead of screws (modular spine distractor). A possible inconvenience of the new device may be its rather bigger frame size compared to others. There are a number of potential advantages of the presented distractor over others currently on the market. This distractor is specific for the lumbar level, and Caspar, e.g., is mostly used for the cervical level. At the lumbar level, the design is focused on the anatomy and functionality of that part of the spine. There are recent publications with objective statistical data which demonstrates the better accuracy, lower surgery time, and RX-exposure reduction when using robotic placement of screws. This is a supporting argument for the calculations carried out. Calculated data of vertebral surface geometry are important when using robots for screw placement. Additionally; for example, Caspar force is usually applied with two fingers. The present distractor has a lever which reduces the physical effort for the surgeon, and also adds precision (that is, a lever not only gives the surgeon more capability to exert a strong force, but also gives him the ability to accurately apply the minimum necessary force) [refs 5-8]. In other words, refinement of the mechanics of operation that could be enhanced with better shape equations for manufacturing. The lever is useful also for long duration operations where many vertebral distractions are necessary, with minimal physical effort. The presented distractor applies the force symmetrically, while Caspar applies force laterally many times. This is an advantage when the vertebra is damaged or deformed. Another potential advantage of the distractor compared to others is its higher range of force, including future designs for even larger forces. This qualifies the distractor for other types of spinal surgery, e.g., difficult spinal deformity operations. We remind the reader that the computational method developed is focused on the screw insertion parallel to endplates of the sagittal plane, but several future applications for spinal tools in contact with vertebral surface are feasible/practical.

To summarize, we presented an improved numerical approximation in CAD for lumbar vertebral bone surface with clinical and bioengineering applications. The discretization method is based on a previous polynomial fitting [refs 5-11], with extent optimal equations. The

refinement constitutes an advance in mathematical-geometrical approximations to obtain more precise vertebral shape equations. In addition, manufacturing/design of spinal surgery instrumentation constitutes an important practical/industrial utility of this study based on human specimens experimental data. A practical surgical spinal distractor design [Casesnoves, Lawson, 2007-8, Appendix 1] corroborates the utility of all modeling and computational work presented.

6.-REFERENCES

- [1] Bertsekas, DP. **Nonlinear Programming**. Second Edition. Athena Scientific. 2003.
- [2] Brinckmann, P, Frobin, W, Leivseth, G. **Muskuloskeletal Biomechanics**. Thieme. 2002.
- [3] Bronstein, AM, Bronstein, MM, Kimmel, R. **Numerical Geometry of Non-Rigid Shapes**. Springer. 2008.
- [4] Buseman, H, Kelly, PJ. **Projective Geometry and Projective Metrics**. Dover Publications, Inc. 2006.
- [5] Casesnoves, F, Lawson, j, and others. “**An Optimization Method for anterior vertebral body morphometry to enhance surgical devices**”. Lecture-Poster. 2008 SIAM Conference of Imaging Science. San Diego CA, USA. July 2008.
- [6] Casesnoves, F. ‘**Computational Simulations of Anterior Vertebral Surface for Statistical Optimization in Surgical Instrumentation Design**’. ASME Peer-reviewed Conference Paper and Poster. Proceedings of the 2010 Design of Medical Devices Conference. April 13-15, 2010, Minneapolis, MN, USA.
- [7] Casesnoves, F. ‘**Computational Simulations of Anterior Vertebral Surface for Statistical Optimization in Surgical Instrumentation Design**’. Peer-Reviewed ASME Conference Paper (American Society of Mechanical Engineers). Proceedings of the 2010 Design of Medical Devices Conference. April 2010, Minneapolis, MN, USA. This paper is included within the Medical Devices Proceedings, and a brief summary in the Official Journal of Medical Devices (print and online). The summary (article main goals and results description) is at: Computational Simulations of the Anterior Vertebral Surface for Optimal Surgical Instrumentation Design. Journal of Medical Devices (Transactions of the ASME) [J. Medical Devices (Trans. ASME)]. Vol. 4, no. 2, 027506 (11pp). Jun 2010.
- [8] Casesnoves, F. ‘**Computational Simulations of Anterior Vertebral Surface for Statistical Optimization in Surgical Instrumentation Design**’. Peer-Reviewed ASME Conference Poster (American Society of Mechanical Engineers). Official Proceedings of 2010 Design of Medical Devices Conference. April 2010, Minneapolis, MN, USA.
- [9] Casesnoves, F. **Computational Simulations of Vertebral Body for Optimal Instrumentation Design**. ASME Journal of Medical Devices (Research Paper). Author: F Casesnoves MSc BSc in Physics, MD, MPhil (Medicine & Surgery). Journal of Medical Devices. June 2012. Volume 6. Issue 2/021014. 11 pages. <http://dx.doi.org/10.1115/1.4006670>.
- [10] Casesnoves, F. ‘**CAD Numerical Vertebral Surface Refinements and Geometrical Data Development for Surgical Devices Design**’. Peer-reviewed Conference Poster. 2013 SIAM Conference on Applied Algebraic Geometry. Fort Collins, Colorado. USA. August 2013. http://meetings.siam.org/session/dsp_talk.cfm?p=59469
- [11] Casesnoves, F. ‘**Geometrical-Computational Inverse Methods for Optimal Geometrical Deformation of Lumbar Artificial Disks Using the Numerical Reuleaux Method**’. Peer-reviewed Poster. SIAM Conference on Geometric & Physical

¹ Tikhonov regularization [refs 20,15.1], originally developed with a Sobolev Norm (Sobolev Spaces), constitutes the base of the nonlinear optimization with least-squares for the mathematical/computational framework of this article. Tikhonov Regularization Theory sets the mathematical framework of modern optimization, complemented by a series of additional remarkable researchers.

Modeling (GD/SPM-13). Denver, Colorado, USA. November 2013. http://meetings.siam.org/sess/dsp_talk.cfm?p=60490.

[12] Chapra, SC, Canale, RP. **Numerical Methods for Engineers**. Fifth Edition. McGraw-Hill. 2006.

[13] Choonsik, L, Lodwick, D, Hasenauer, D, Williams, JL, Choonik, L, Bolch, WE. "Hybrid computational phantoms of male and female newborn patient: NURBS-based whole-body models". *Phys Med Biol*. Vol 52, Issue 12. 2007.

[14] Fausett, LV. **Applied Numerical Analysis using Matlab**. Second Edition. Pearson. 2008.

[15] Fischer, B, Haber, E, Modersitzki, J. "Mathematics Meets Medicine-An Optimal Alignment". *SIAG/OPT Views-and-News*. SIAM Publications. Volume 19, Number 2. 2008.

[15.1] Hanke, M, and colls "Regularization of inverse problems", *Kluwer Acad. Publ* (1996) MR1408680 Zbl 0859.65054 260

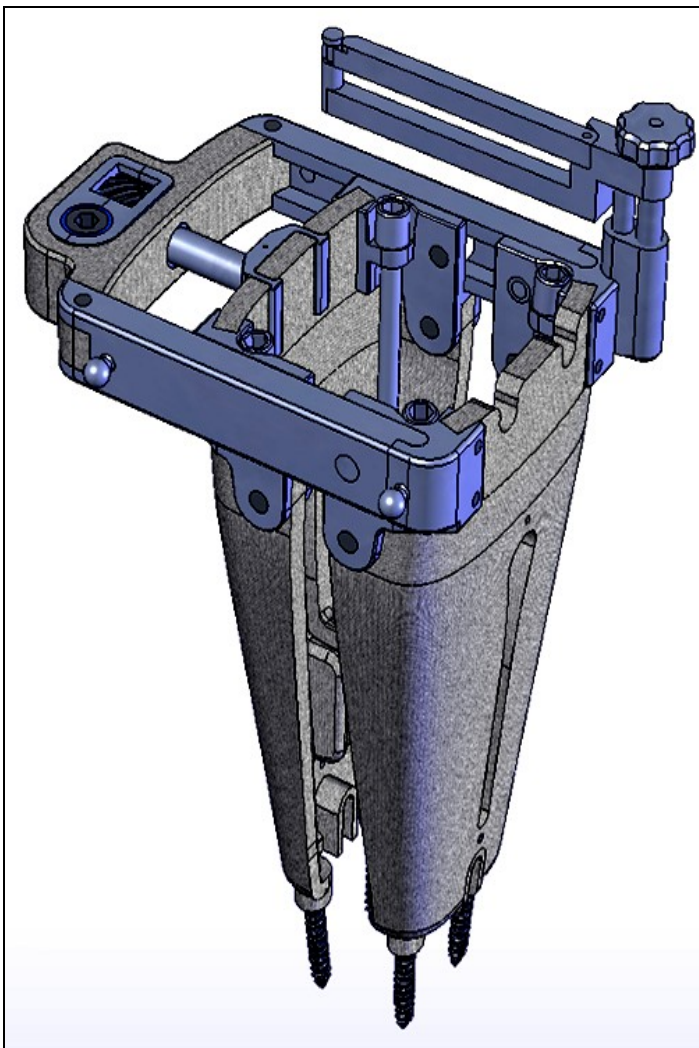
[16] Hildebrand, FB. **Introduction to Numerical Analysis**. Second Edition. Dover Publications, Inc. 1987.

[17] Jennings, GA. **Modern Geometry with Applications**. Springer. 1994.

[18] Kim, DH, Camisa, FP, Fessler, RG. **Dynamic Reconstruction of the Spine**. Thieme New York. 2006.

[19] Kirsch, A. **An Introduction to the Mathematical Theory of Inverse Problems**. Springer, Applied Mathematical Sciences. Volume 120. 1996.

[20] Tikhonov, A.N. "Solution of incorrectly formulated problems and the regularization method" *Soviet Math. Dokl.*, 4 (1963) pp. 1035-1038 MR0211218 Zbl 0141.11001

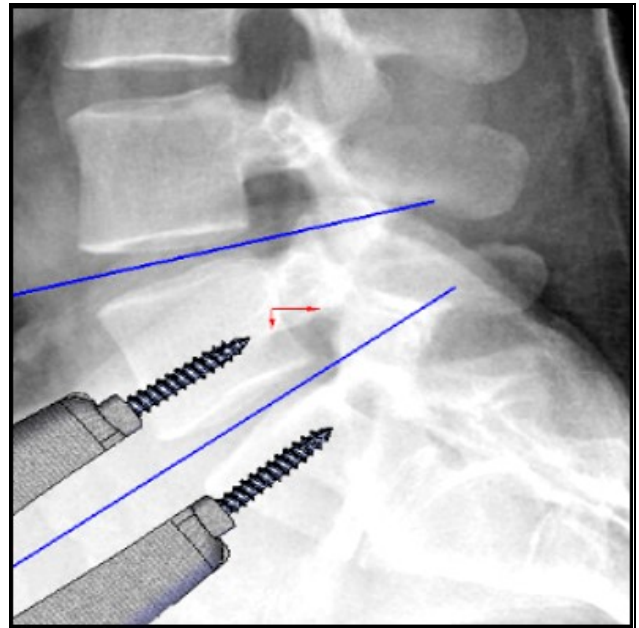
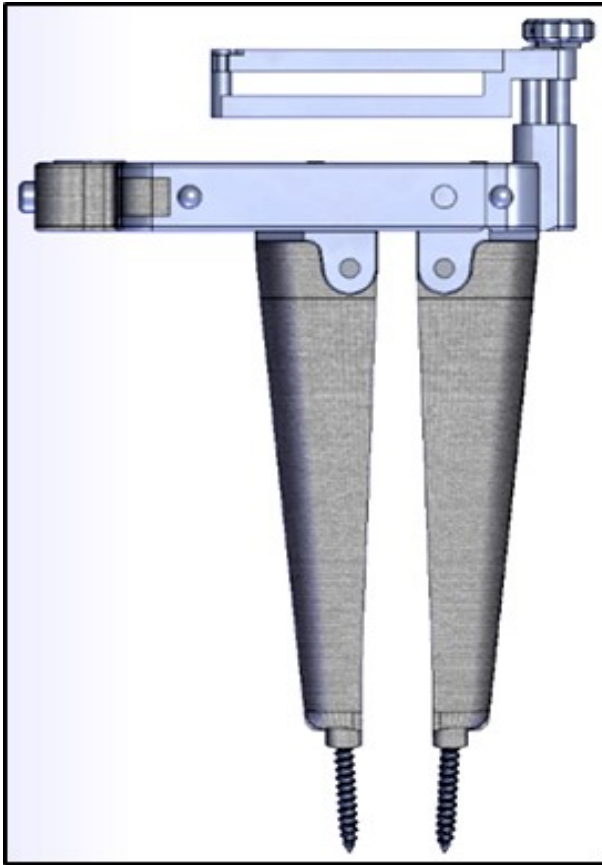


7.-APPENDICES

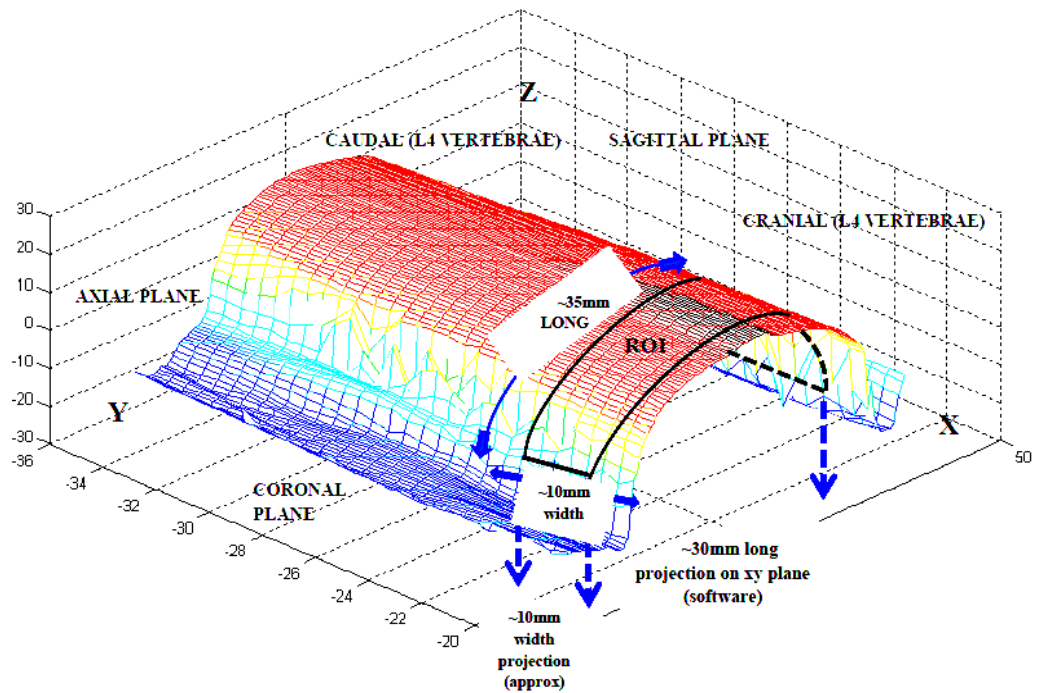
Appendix 1.-Table of Vertebral-Shape Equations from [refs 6-9] and principal distractor frame. Funcional sketches done with computational-engineering design software for the spinal distractor designed theoretically by F Casesnoves (2007, refs [8,9]) and implemented in images by Jonathan Lawson in 2008. The radiographic simulation of the distractor lumbar insertion in L4-5 is also pictured. This medical device has been mechanically improved with new variations/applications [Casesnoves, 2013], and will constitute complementary subject of further outcoming contributions.



Coefficients, equations, and method	$z^2 + a(1)z = a(2) + a(3)x + a(4)x^2 + a(5)y + a(6)y^2$ Interior-Reflective Newton Method							
	$z_1(x, y) = (k_1 + k_2x + k_3x^2 + k_4y + k_5y^2)^{1/2} = (z - z_0)$ Optimization Algorithm:							
Vertebra and surface	a(1)	a(2)	a(3), K ₂	a(4), K ₃	a(5), K ₄	a(6), K ₅	Z ₀	K ₁
L3 UPPER	-21.0±15.1	3.5±27.6	2.0±15	0.0± 0.4	-0.1±4.1	-0.2±0.4	-10.5±7.5	130±120
L3 LOWER	-21.2±16.6	6.5±33.8	3.6±18	0.0± 0.4	0.1±4.3	-0.2±0.4	-10.6±8.3	150±190
L4 UPPER	-32.2±18.3	-150.9±370.9	-2.1±7	0.3±0.4	0.9±5.1	-0.2±0.4	-16.1±9.1	130±250
L4 LOWER	-32.5±16.8	-151.2±291.9	-2.5±19	0.3±0.3	0.8±4.5	-0.2±0.3	-16.2±8.4	130±260
L5 UPPER	-35.0±12.7	-15.7±30.2	-11.4±12.8	0.1±0.2	-0.0±4.0	-0.1±0.4	-17.5±6.8	300±230
L5 LOWER	-35.4±13.0	-16.5±36.2	-11.5±18.2	0.1±0.3	-0.5±4.6	-0.1±0.4	-17.8±7.3	310±210
S1 UPPER	-14.0±25.8	9.8±74.7	1.3±4.5	-0.0±0.7	-0.5±4.0	-0.0±0.4	-7.9±12.8	110±160



Appendix 2.-Polynomial-surface/curve projection for geometrical optimization [from refs. 6-9]. The vertebral surface is real from a human specimen, and the mathematical sketches are included over the original image.



After the selection of the limits of this ROI, taking the Z Coordinate and X, Y Coordinates projections at XY plane, we extract a numerical matrix to carry out the Optimization mainly with this Algorithm,

$$\sum_{i=1}^N \left\| (z_i^2 + k_1 z_i) - (k_2 + k_3 x_i + k_4 x_i^2 + k_5 y_i + k_6 y_i^2) \right\|^2$$